Hydrothermal Syntheses and Structural Characterizations of Organic−Inorganic Hybrid Materials of the M(II)−Ligand/Vanadium Oxide System (M(II) = Cu(II) and Zn(II); Ligand = 2,2′-Bipyridine and 2,2′:6′,2″-Terpyridine)

Pamela J. Hagrman and Jon Zubieta*

Department of Chemistry, Syracuse University, Syracuse, New York 13244

Received January 5, 2001

Investigation into the incorporation of complex transition metal−organic units into vanadium oxide structures has resulted in the preparation of several novel composite materials. Hydrothermal reactions of V_2O_5, 2,2′-bipyridine, an appropriate Zn or Cu starting material, and H_2O under a variety of conditions yielded the organic−inorganic hybrid materials $[\{Zn(2,2'\text{-bpy})\}_2V_4O_{12}]$ (**1**) and $[Cu(2,2'\text{-bpy})V_4O_{10.5}]$ (**2**). Blocking an additional coordination site on the secondary metal center by using a tridentate organonitrogen ligand, 2,2′:6′,2″-terpyridine in place of 2,2′-bipyridine, allowed the isolation of $[Cu(terpy)V_2O_6]$ (**3**) and $[\{Zn(terpy)\}_2V_6O_{17}]$ (**4**). The structure of **1** is a two-dimensional zinc vanadate layer, composed of rings containing four corner-sharing $\{VO_4\}$ vanadium(V) tetrahedra linked through six zinc square pyramids, with the 2,2′-bipyridine groups attached to the zinc centers and directed above and below the plane of the layer. In contrast to **1**, the layer of **2** is based on a two-dimensional vanadium oxide substructure composed of vanadium(IV) square pyramids and vanadium(V) tetrahedra with copper square pyramids attached through corner-sharing interactions with vanadium tetrahedra such that the bipyridine ligands attached to the copper sites form staggered stacks above and below the plane of the layer. Compound **3** consists of one-dimensional vanadium oxide chains of corner-sharing tetrahedra linked through copper−terpyridine units into a two-dimensional bimetallic oxide of composition $\{CuV_2O_6\}$, while the layer structure of **4** contains more complex one-dimensional vanadium oxide chains composed of fused rings of six corner-sharing vanadium oxide tetrahedra which are linked into a layer through $\{Zn(terpy)\}^{2+}$ units.

Introduction

The contemporary widespread interest in metal oxide based solid phases derives from their potential applications in such diverse areas as catalysis, ion exchange, sorption, energy storage, molecular electronics, and optical materials.[1,2] Exploitation of hydrothermal techniques in combination with the introduction of organic components possessing structure-directing properties has allowed the isolation of a remarkable array of metastable inorganic/organic composite oxides which retain some structural features of their synthetic precursors.[3,4] Typically, the organic substituents have been present as charge-compensating cations, such as organoammonium units. Examples of such compounds include the one-dimensional $[H_3NCH_2CH_2NH_3][Mo_3O_{10}]$[5] and $[H_3N(CH_2)_6NH_3][Mo_4O_{13}]$[6] and the two-dimensional phases $[4,4'\text{-}H_2bpy][Mo_7O_{22}]\cdot H_2O$,[7] $[H_3N(CH_2)_3NH_3][V_4O_{10}]$,[8] and $[HN(C_2H_4)_3NH][V_6O_{14}]\cdot H_2O$.[9]

Alternatively, the organic substituents have been introduced as ligands covalently linked to the inorganic backbone of a metal oxide solid. Such materials include the one-dimensional vanadium oxide phases $[VO(VO_3)_6\{VO(2,2'\text{-bpy})_2\}_2]$ [10] and $[V^{IV}V^{V}{}_2O_7(phen)]_n$,[11] and the three related one-dimensional molybdenum oxide phases $[MoO_3(2,2'\text{-bpy})]$, $[Mo_2O_6(2,2'\text{-bpy})]$, and $[Mo_3O_9(2,2'\text{-bpy})_2]$.[12] Another mode of ligation observed for these ligands is as "tethers" between metal sites, a modality commonly adopted by 4,4′-bipyridine in materials such as $[MoO_3(4,4'\text{-bpy})_{0.5}]$,[13] for example.

Exploitation of amine-ligated transition metal complex cations as building blocks in the construction of metal oxide composite materials is another strategy which has proved fruitful. The most common manifestation of such subunits is as molecular cations with no covalent attachment to the metal oxide substructure of the material, that is, as charge-compensating components sandwiched between metal oxide sheets. Examples of complex transition metal−organic subunits as interlamellar moieties include $[(en)_2Zn][V_6O_{14}]$, $[(en)_2Cu][V_6O_{14}]$, and $[(en)_2Cu]_2[V_{10}O_{25}]$ (en = ethylenediamine).[14] Recently, a family of materials in which a unit composed of a bidentate amine attached to a secondary transition metal which is directly incorporated into the metal oxide backbone has been described. In the specific case of the molybdenum oxide systems, a wide variety of composite materials was accessed, ranging from binuclear $[Mo_2O_7]^{2-}$ units bridged by $[Ni(2,2'\text{-bpy})_2]^{2+}$ groups into a $[Ni_2Mo_4]$ cluster,[15] to isolated $\{Mo_8O_{26}\}^{4-}$

(1) Cheetham, A. J. *Science* **1994**, *264*, 794 and references therein.
(2) Cox, P. A. *Transition Metal Oxides*; Clarendon Press: Oxford, England, 1995.
(3) Gopalikrishnan, J. *Chem. Mater.* **1995**, *7*, 1265.
(4) Hagrman, P. J.; Hagrman, D.; Zubieta, J. *Angew. Chem., Int. Ed.* **1999**, *38*, 2638.
(5) Khan, M. I.; Chen, Q.; Zubieta, J. *Inorg. Chim. Acta* **1993**, *213*, 325.
(6) Xu, Y.; An, L.-H.; Koh, L.-L. *Chem. Mater.* **1996**, *8*, 814.
(7) Zapf, P. J.; Haushalter, R. C.; Zubieta, J. *Chem. Commun.* **1997**, 321.
(8) Zhang, Y.; O'Connor, C. J.; Clearfield, A.; Haushalter, R. C. *Chem. Mater.* **1996**, *8*, 595.
(9) Zhang, Y.; Clearfield, A.; Haushalter, R. C. *Chem. Commun.* **1996**, 1055.
(10) Guohne, H.; Johnson, J. W.; Jacobson, A. J.; Merola, J. S. *J. Solid State Chem.* **1991**, *91*, 385.
(11) Duan, C.-Y.; Tian, Y.-P.; Lu, Z.-L.; You, X.-Z. *Inorg. Chem.* **1995**, *34*, 1.
(12) Zapf, P. J.; Haushalter, R. C.; Zubieta, J. *Chem. Mater.* **1997**, *9*, 2019.
(13) Hagrman, P. J.; LaDuca, R. L., Jr.; Hoo, H.-J.; Rarig, R., Jr.; Haushalter, R. C.; Whangbo, M.-H.; Zubieta, J. *Inorg. Chem.* **2000**, *39*, 4511.
(14) Zhang, Y.; DeBord, J. R. D.; O'Connor, C. J.; Haushalter, R. C.; Clearfield, A.; Zubieta, J. *Angew. Chem., Int. Ed. Engl.* **1996**, *35*, 989.

10.1021/ic010024m CCC: $20.00
Published on Web 05/03/2001

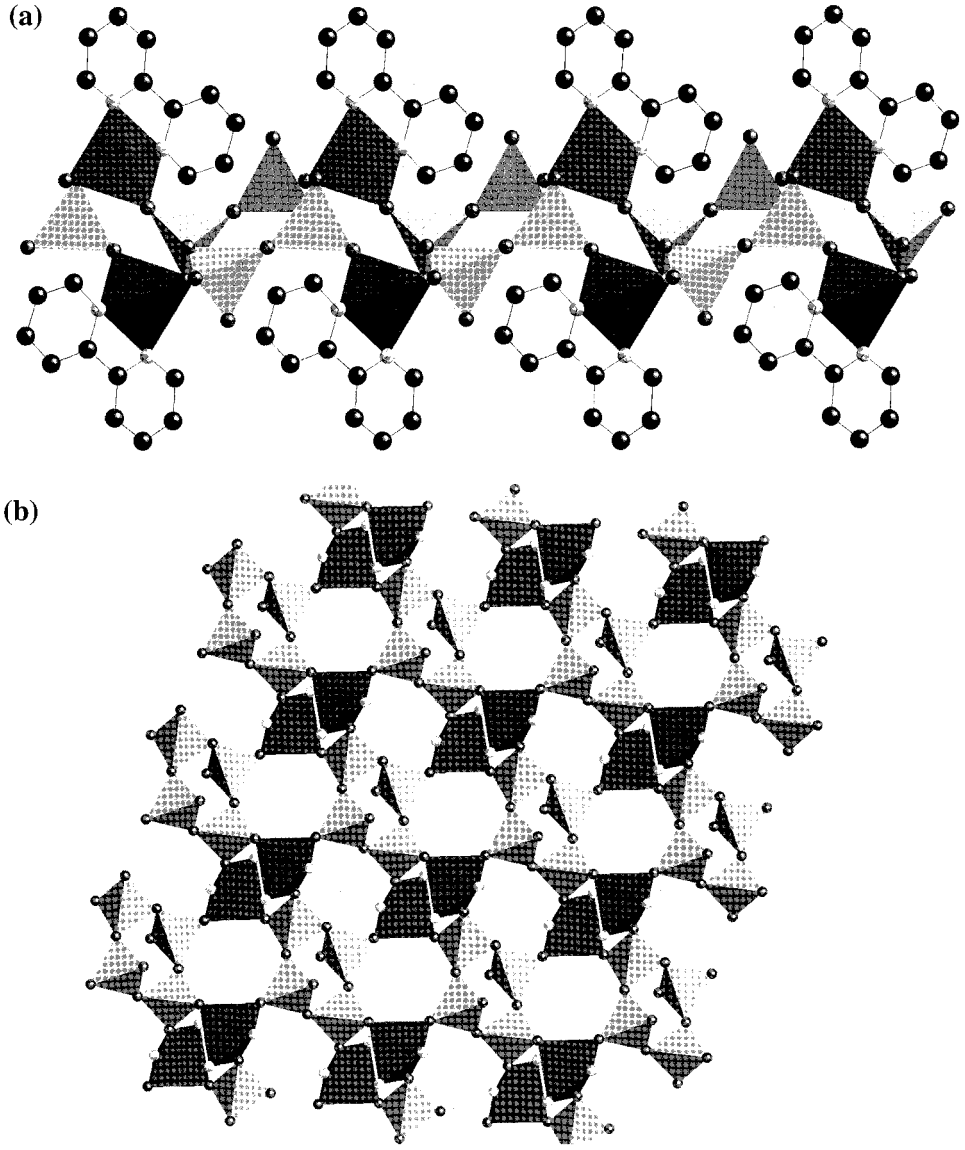

Figure 1. Polyhedral view of the structure of **1** (a) down the crystallographic *b* axis and (b) along *c* showing the zinc vanadate layer with the carbon and hydrogen atoms of the 2,2′-bipyridine ligand omitted for clarity. Vanadium sites are light gray shaded polyhedra, zinc polyhedra are shown in dark gray, nitrogen atoms are light gray spheres, carbon atoms are black spheres, and oxygen atoms are dark gray spheres. This convention in maintained throughout, except as otherwise noted.

Table 1. Crystallographic Data for Zn(2,2′-bpy)[V_2O_6] (**1**), Cu(2,2′-bpy)[$V_4O_{10.50}$] (**2**), Cu(terpy)[V_2O_6] (**3**), and [V_6O_{17}{Zn(terpy)}$_2$] (**4**)

	1	**2**	**3**	**4**
empirical formula	$C_{10}H_8N_2O_6V_2Zn$	$C_{10}H_8CuN_2O_{10.50}V_4$	$C_{15}H_{11}CuN_3O_6V_2$	$C_{30}H_{22}N_6O_{17}V_6Zn_2$
fw	419.43	591.48	494.69	1174.92
space group	*P*1	*P*1	*Pbca*	*P*1
a (Å)	8.0597(6)	8.0679(2)	16.2789(4)	9.6981(8)
b (Å)	8.2040(6)	9.6449(3)	10.5658(3)	10.1729(9)
c (Å)	10.2850(8)	11.6379(3)	18.8712(5)	11.1223(10)
α (deg)	72.184(1)	85.648(1)	90	66.556(2)
β (deg)	84.180(1)	72.627(1)	90	81.654(2)
γ (deg)	76.625(1)	72.734(1)	90	74.412(2)
V (Å)	629.54(8)	825.25(4)	3245.84(15)	968.78(15)
Z	2	2	8	1
D_{calcd} (g/cm^3)	2.213	2.380	2.025	2.014
μ (mm^{-1})	3.372	3.509	2.468	2.678
T (K)	120(2)	120(2)	96(2)	96(2)
λ (Å)	0.71073	0.71073	0.71073	0.71073
final R1,[a] wR2[b] [$I > 2\sigma(I)$]	0.0285, 0.0683	0.0303, 0.0635	0.0513, 0.0801	0.0313, 0.0731
final R1,[a] wR2[b] (all data)	0.0320, 0.0706	0.0430, 0.0680	0.0933, 0.0906	0.0374, 0.0754

[a] $R1 = \sum||F_o| - |F_c||/\sum|F_o|$. [b] $wR2 = [\sum[w(F_o^2 - F_c^2)^2]/\sum[w(F_o^2)^2]]^{1/2}$.

molybdenum oxide clusters linked into a one-dimensional chain through {Ni(2,2′-bpy)$_2$}$^{2+}$ units which bridge adjacent clusters in [Ni(2,2′-bpy)$_2$Mo$_4$O$_{13}$],[16] to molybdenum oxide chains with peripheral {Cu(2,2′-bpy)}$^{2+}$ moieties as observed for [Cu(2,2′-bpy)Mo$_2$O$_7$][16] and [Cu(2,2′-bpy)Mo$_4$O$_{13}$],[17] to compounds constructed from molybdenum oxide ribbons linked through {Co(2,2′-bpy)}$^{2+}$ units into infinite sheets as seen in [Co(2,2′-bpy)Mo$_3$O$_{10}$].[16] Furthermore, compounds in which discrete {MoO$_4$}$^{2-}$ or {Mo$_2$O$_7$}$^{2-}$ units are linked into one-dimensional chains through {Fe(2,2′-bpy)}$^{3+}$ bridging units,

Table 2. Selected Bond Lengths and Angles for **1**−**4**

[{Zn(2,2′-bpy)}$_2$V$_4$O$_{12}$] (**1**)

Zn(1)−O(7)	2.0126(19)	V(3)−O(6)	1.7745(18)	O(3)#1−Zn(1)−N(2)	85.46(8)	O(4)−V(3)−O(6)	108.10(9)
Zn(1)−O(4)	2.0176(19)	V(3)−O(5)#3	1.7787(19)	N(1)−Zn(1)−N(2)	78.65(8)	O(3)−V(3)−O(5)#3	108.91(9)
Zn(1)−O(3)#1	2.0371(19)			O(2)−V(2)−O(7)	108.85(10)	O(4)−V(3)−O(5)#3	110.57(9)
Zn(1)−N(1)	2.082(2)	O(7)−Zn(1)−O(4)	94.24(8)	O(2)−V(2)−O(6)#2	109.30(10)	O(6)−V(3)−O(5)#3	109.60(9)
Zn(1)−N(2)	2.116(2)	O(7)−Zn(1)−O(3)#1	89.19(7)	O(7)−V(2)−O(6)#2	112.30(9)	V(2)−O(7)−Zn(1)	158.07(12)
V(2)−O(2)	1.6158(19)	O(4)−Zn(1)−O(3)#1	120.53(8)	O(2)−V(2)−O(5)	108.88(10)	V(3)−O(6)−V(2)#2	160.86(12)
V(2)−O(7)	1.6685(19)	O(7)−Zn(1)−N(1)	100.39(8)	O(7)−V(2)−O(5)	109.44(9)	V(3)#4−O(5)−V(2)	137.62(11)
V(2)−O(6)#2	1.8090(19)	O(4)−Zn(1)−N(1)	111.56(8)	O(6)#2−V(2)−O(5)	108.01(9)	V(3)−O(4)−Zn(1)	130.30(10)
V(2)−O(5)	1.8144(19)	O(3)#1−Zn(1)−N(1)	126.09(8)	O(3)−V(3)−O(4)	108.87(10)	V(3)−O(3)−Zn(1)#1	162.12(12)
V(3)−O(3)	1.6496(19)	O(7)−Zn(1)−N(2)	172.47(8)	O(3)−V(3)−O(6)	110.78(9)		
V(3)−O(4)	1.6727(18)	O(4)−Zn(1)−N(2)	93.05(8)				

symmetry transformations used to generate equivalent atoms: #1 $-x+1, -y+2, -z$; #2 $-x, -y+2, -z$; #3 $x, y+1, z$; #4 $x, y-1, z$

[Cu(2,2′-bpy)V$_4$O$_{10.5}$] (**2**)

Cu(1)−O(3)	1.941(2)	V(5)−O(7)#2	1.694(2)	O(11)−V(2)−O(10)	108.59(11)	O(1)#2−V(5)−O(7)#2	107.26(12)
Cu(1)−O(2)	1.956(2)	V(5)−O(10)	1.753(2)	O(9)−V(2)−O(10)	107.74(11)	O(1)#2−V(5)−O(10)	110.69(12)
Cu(1)−N(1)	1.979(3)	V(5)−O(4)#3	1.799(2)	O(2)−V(3)−O(6)	109.35(12)	O(7)#2−V(5)−O(10)	111.71(11)
Cu(1)−N(2)	1.996(3)			O(2)−V(3)−O(4)	111.37(11)	O(1)#2−V(5)−O(4)#3	108.61(11)
Cu(1)−O(1)	2.245(2)	O(3)−Cu(1)−O(2)	91.39(10)	O(6)−V(3)−O(4)	107.96(11)	O(7)#2−V(5)−O(4)#3	109.74(11)
V(2)−O(3)	1.669(2)	O(3)−Cu(1)−N(1)	94.85(10)	O(2)−V(3)−O(5)	108.66(8)	O(10)−V(5)−O(4)#3	108.77(11)
V(2)−O(11)	1.691(2)	O(2)−Cu(1)−N(1)	170.40(10)	O(6)−V(3)−O(5)	110.97(8)	V(5)#4−O(1)−Cu(1)	136.28(13)
V(2)−O(9)	1.694(2)	O(3)−Cu(1)−N(2)	166.83(10)	O(4)−V(3)−O(5)	108.53(8)	V(3)−O(2)−Cu(1)	142.71(14)
V(2)−O(10)	1.811(2)	O(2)−Cu(1)−N(2)	90.20(10)	O(8)−V(4)−O(9)	107.61(11)	V(2)−O(3)−Cu(1)	153.76(14)
V(3)−O(2)	1.646(2)	N(1)−Cu(1)−N(2)	82.08(11)	O(8)−V(4)−O(11)#1	103.26(11)	V(3)−O(4)−V(5)#3	141.19(14)
V(3)−O(6)	1.664(2)	O(3)−Cu(1)−O(1)	94.64(9)	O(9)−V(4)−O(11)#1	86.58(9)	V(3)−O(5)−V(3)#3	180.00(3)
V(3)−O(4)	1.772(2)	O(2)−Cu(1)−O(1)	90.54(9)	O(8)−V(4)−O(7)	107.47(11)	V(3)−O(6)−V(4)	155.80(15)
V(3)−O(5)	1.7793(5)	N(1)−Cu(1)−O(1)	96.20(10)	O(9)−V(4)−O(7)	144.83(10)	V(5)#4−O(7)−V(4)	120.50(13)
V(IV)(4)−O(8)	1.593(2)	N(2)−Cu(1)−O(1)	98.42(10)	O(11)#1−V(4)−O(7)	87.92(10)	V(2)−O(9)−V(4)	144.69(14)
V(IV)(4)−O(9)	1.938(2)	O(3)−V(2)−O(11)	110.12(12)	O(8)−V(4)−O(6)	100.15(11)	V(5)−O(10)−V(2)	165.77(15)
V(IV)(4)−O(11)#1	1.939(2)	O(3)−V(2)−O(9)	110.35(11)	O(9)−V(4)−O(6)	85.60(9)	V(2)−O(11)−V(4)#1	154.12(14)
V(IV)(4)−O(7)	1.960(2)	O(11)−V(2)−O(9)	110.08(11)	O(11)#1−V(4)−O(6)	156.58(11)		
V(IV)(4)−O(6)	2.000(2)	O(3)−V(2)−O(10)	109.90(11)	O(7)−V(4)−O(6)	85.86(9)		
V(5)−O(1)#2	1.632(2)						

symmetry transformations used to generate equivalent atoms: #1 $-x, -y+1, -z+1$; #2 $x-1, y, z$; #3 $-x, -y+1, -z$; #4 $x+1, y, z$

[Cu(terpy)V$_2$O$_6$] (**3**)

Cu(1)−O(5)#1	1.919(3)	V(2)−O(5)	1.712(3)	O(5)#1−Cu(1)−O(6)	96.96(11)	O(4)−V(2)−O(5)	109.14(14)
Cu(1)−N(2)	1.930(3)	V(2)−O(2)	1.778(3)	N(2)−Cu(1)−O(6)	91.47(12)	O(4)−V(2)−O(2)	109.55(14)
Cu(1)−N(1)	2.031(3)	V(2)−O(3)	1.792(3)	N(1)−Cu(1)−O(6)	91.94(11)	O(5)−V(2)−O(2)	109.67(13)
Cu(1)−N(3)	2.049(3)			N(3)−Cu(1)−O(6)	86.93(11)	O(4)−V(2)−O(3)	109.11(14)
Cu(1)−O(6)	2.369(3)	O(5)#1−Cu(1)−N(2)	171.02(13)	O(1)−V(1)−O(6)#1	108.42(15)	O(5)−V(2)−O(3)	108.20(13)
V(1)−O(1)	1.637(3)	O(5)#1−Cu(1)−N(1)	96.51(12)	O(1)−V(1)−O(3)#2	109.28(13)	O(2)−V(2)−O(3)	111.14(13)
V(1)−O(6)#1	1.648(3)	N(2)−Cu(1)−N(1)	80.05(13)	O(6)#1−V(1)−O(3)#2	109.72(14)	V(2)−O(2)−V(1)	128.91(16)
V(1)−O(3)#2	1.799(3)	O(5)#1−Cu(1)−N(3)	103.21(12)	O(1)−V(1)−O(2)	108.43(14)	V(2)−O(3)−V(1)#3	139.92(17)
V(1)−O(2)	1.831(3)	N(2)−Cu(1)−N(3)	80.26(14)	O(6)#1−V(1)−O(2)	109.06(14)	V(2)−O(5)−Cu(1)#1	134.75(16)
V(2)−O(4)	1.613(3)	N(1)−Cu(1)−N(3)	160.24(13)	O(3)#2−V(1)−O(2)	111.86(13)	V(1)#1−O(6)−Cu(1)	119.39(14)

symmetry transformations used to generate equivalent atoms: #1 $-x, -y, -z$; #2 $-x-{}^1/_2, y-{}^1/_2, z$; #3 $-x-{}^1/_2, y+{}^1/_2, z$

[V$_6$O$_{17}${Zn(terpy)}$_2$] (**4**)

Zn(1)−O(14)	1.967(4)	V(5)−O(10)	1.607(4)	O(12)−Zn(2)−N(6)	94.82(19)	O(11)−V(4)−O(3)	109.2(2)
Zn(1)−O(8)	1.970(4)	V(5)−O(12)	1.676(4)	N(5)−Zn(2)−N(6)	75.86(19)	O(13)−V(4)−O(3)	109.23(19)
Zn(1)−N(2)	2.065(5)	V(5)−O(7)	1.790(4)	N(4)−Zn(2)−N(6)	152.36(18)	O(10)−V(5)−O(12)	108.9(2)
Zn(1)−N(3)	2.165(5)	V(5)−O(6)	1.831(4)	O(17)−V(1)−O(6)	109.3(2)	O(10)−V(5)−O(7)	109.1(2)
Zn(1)−N(1)	2.170(5)	V(6)−O(2)	1.604(4)	O(17)−V(1)−O(3)#1	108.7(2)	O(12)−V(5)−O(7)	110.8(2)
Zn(2)−O(11)	1.961(4)	V(6)−O(14)	1.670(4)	O(6)−V(1)−O(3)#1	111.6(2)	O(10)−V(5)−O(6)	108.9(2)
Zn(2)−O(12)	1.971(4)	V(6)−O(7)	1.786(4)	O(17)−V(1)−O(16)	109.9(2)	O(12)−V(5)−O(6)	110.6(2)
Zn(2)−N(5)	2.062(5)	V(6)−O(4)	1.842(4)	O(6)−V(1)−O(16)	107.54(19)	O(7)−V(5)−O(6)	108.5(2)
Zn(2)−N(4)	2.157(5)			O(3)#1−V(1)−O(16)	109.9(2)	O(2)−V(6)−O(14)	109.0(2)
Zn(2)−N(6)	2.172(5)	O(14)−Zn(1)−O(8)	105.80(17)	O(15)−V(2)−O(5)	109.0(2)	O(2)−V(6)−O(7)	108.5(2)
V(1)−O(17)	1.601(4)	O(14)−Zn(1)−N(2)	134.74(19)	O(15)−V(2)−O(4)#2	109.0(2)	O(14)−V(6)−O(7)	111.9(2)
V(1)−O(6)	1.735(5)	O(8)−Zn(1)−N(2)	119.01(18)	O(5)−V(2)−O(4)#2	109.7(2)	O(2)−V(6)−O(4)	110.0(2)
V(1)−O(3)#1	1.743(4)	O(14)−Zn(1)−N(3)	102.02(19)	O(15)−V(2)−O(16)#3	106.97(18)	O(14)−V(6)−O(4)	108.2(2)
V(1)−O(16)	1.789(4)	O(8)−Zn(1)−N(3)	101.65(18)	O(5)−V(2)−O(16)#3	110.90(19)	O(7)−V(6)−O(4)	109.2(2)
V(2)−O(15)	1.604(4)	N(2)−Zn(1)−N(3)	76.08(19)	O(4)#2−V(2)−O(16)#3	111.3(2)	V(1)#2−O(3)−V(4)	139.4(2)
V(2)−O(5)	1.737(4)	O(14)−Zn(1)−N(1)	93.50(18)	O(9)−V(3)−O(8)	108.4(2)	V(2)#1−O(4)−V(6)	139.2(3)
V(2)−O(4)#2	1.748(4)	O(8)−Zn(1)−N(1)	96.68(18)	O(9)−V(3)−O(13)	109.2(2)	V(2)−O(5)−V(3)	138.6(2)
V(2)−O(16)#3	1.785(4)	N(2)−Zn(1)−N(1)	76.12(19)	O(8)−V(3)−O(13)	112.0(2)	V(1)−O(6)−V(5)	155.2(3)
V(3)−O(9)	1.610(4)	N(3)−Zn(1)−N(1)	151.62(18)	O(9)−V(3)−O(5)	108.9(2)	V(6)−O(7)−V(5)	150.1(3)
V(3)−O(8)	1.671(4)	O(11)−Zn(2)−O(12)	109.52(17)	O(8)−V(3)−O(5)	111.00(19)	V(3)−O(8)−Zn(1)	131.5(2)
V(3)−O(13)	1.782(4)	O(11)−Zn(2)−N(5)	136.77(19)	O(13)−V(3)−O(5)	107.3(2)	V(4)−O(11)−Zn(2)	132.8(2)
V(3)−O(5)	1.840(4)	O(12)−Zn(2)−N(5)	113.32(18)	O(1)−V(4)−O(11)	109.4(2)	V(5)−O(12)−Zn(2)	127.1(2)
V(4)−O(1)	1.611(4)	O(11)−Zn(2)−N(4)	101.74(18)	O(1)−V(4)−O(13)	109.0(2)	V(3)−O(13)−V(4)	144.0(3)
V(4)−O(11)	1.674(4)	O(12)−Zn(2)−N(4)	99.67(18)	O(11)−V(4)−O(13)	110.4(2)	V(6)−O(14)−Zn(1)	132.8(2)
V(4)−O(13)	1.792(4)	N(5)−Zn(2)−N(4)	76.81(19)	O(1)−V(4)−O(3)	109.6(2)	V(2)#4−O(16)−V(1)	140.4(2)
V(4)−O(3)	1.840(4)	O(11)−Zn(2)−N(6)	95.33(18)				

symmetry transformations used to generate equivalent atoms: #1 $x, y-1, z$; #2 $x, y+1, z$; #3 $x+1, y+1, z$; #4 $x-1, y-1, z$

of which [Mo$_4$O$_{15}${Fe^{III}(2,2′-bpy)}][18] is representative, have also been observed.

A logical extension of this diverse molybdenum oxide chemistry was a parallel investigation of the incorporation of transition metal−organic subunits into vanadium oxide solids. While initial forays into the chemistry of this family of materials have produced such compounds as [{Zn(2,2′-bpy)$_2$}$_2$V$_6$O$_{17}$][14] and [{M(2,2′-bpy)}$_2$V$_{12}$O$_{32}$] (M = Co, Cu, Ni),[19] the wide variety of materials observed in the molybdenum oxide system led us to anticipate that additional phases should be manifested

(15) Zhang, Y.; Zapf, P. J.; Meyer, L. M.; Haushalter, R. C.; Zubieta, J. *Inorg. Chem.* **1997**, *36*, 2159.
(16) Zapf, P. J.; Warren, C. J.; Haushalter, R. C.; Zubieta. J. *Chem. Commun.* **1997**, 1543.
(17) Hagrman, P. J., Hagrman, D.; Zubieta, J. *Angew. Chem., Int. Ed.* **1999**, *38*, 2639.
(18) Zapf, P. J.; Hammond, R. P.; Haushalter, R. C.; Zubieta, J. *Chem. Mater*. **1998**, *10*, 1366.

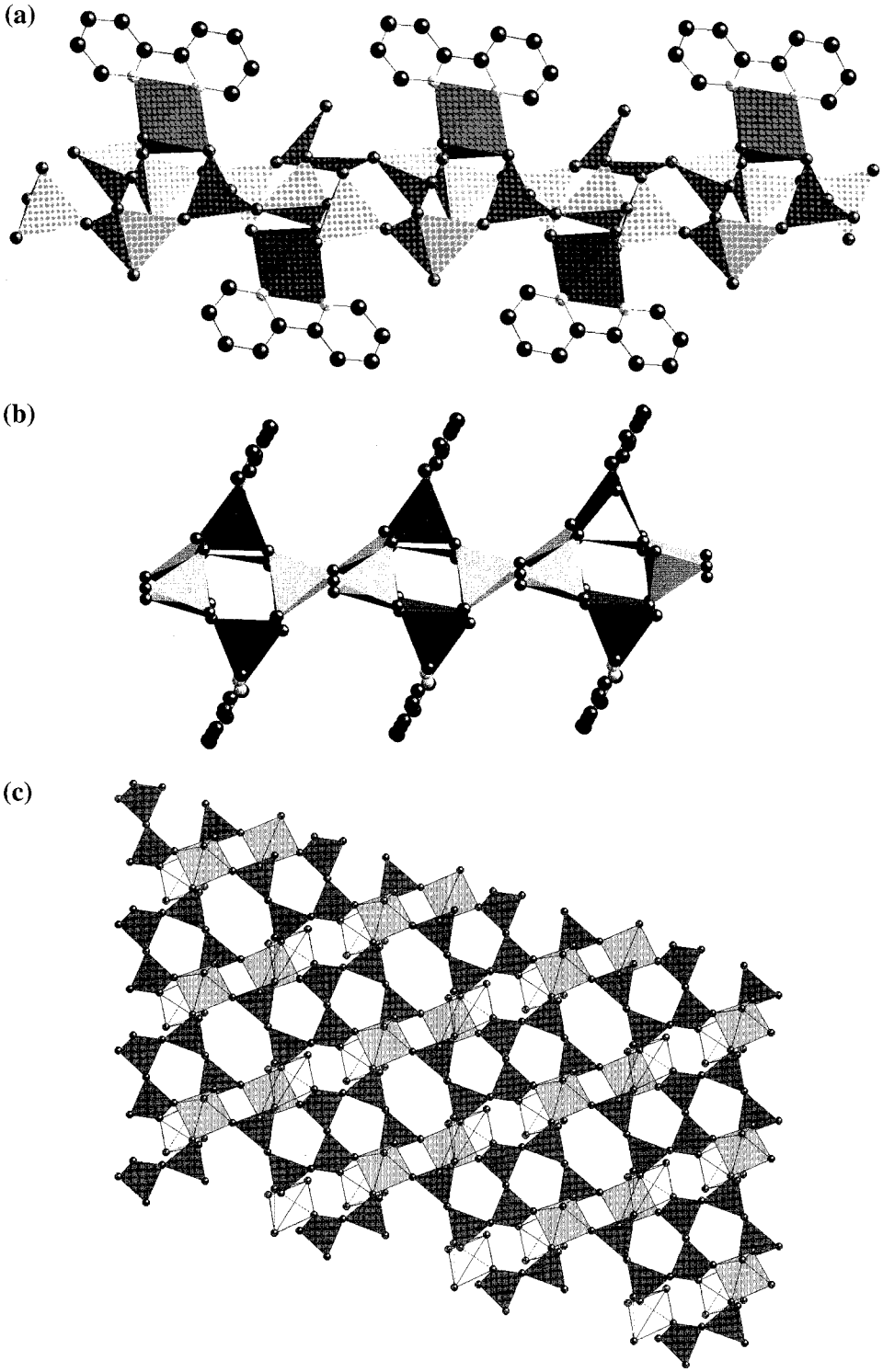

Figure 2. The structure of **2** shown using polyhedral representations (a) as viewed along the crystallographic *a* axis, (b) illustrating the orientation of the 2,2′-bipyridine groups with respect to the layer, and (c) viewed along *b*, showing the copper vanadate layer with copper polyhedra in outline form, vanadium square pyramids in light gray and vanadium tetrahedra in dark gray.

in the vanadium oxide chemistry. Furthermore, while the previously reported vanadium oxide structures incorporating complex transition metal−organic subunits were exclusively based on two-dimensional vanadium oxide building blocks, in the molybdenum oxide materials it has been observed that molecular building blocks were commonly integrated into the structure, as noted for $[Ni(2,2'\text{-bpy})_2Mo_4O_{13}]$[16] and $[Mo_4O_{15}\{Fe^{III}(2,2'\text{-bpy})\}]$ and also in $[MoO_4\{Fe^{III}Cl(2,2'\text{-bpy})\}]$ and $[Mo_3O_{12}\{Fe^{III}(2,2'\text{-bpy})\}_2]$.[18] Consequently, attempts were made to synthesize higher dimensionality materials consisting of complex transition metal−organonitrogen units and vanadium oxide building blocks of various dimensionalities and nuclearities.

This study of the incorporation of complex transition metal−organic units into vanadium oxide structures has resulted in the preparation of several novel composite materials. When 2,2′-

(19) Ollivier, P. J.; DeBord, J. R. D.; Zapf, P. J.; Zubieta, J.; Meyer, L. M.; Wang, C.-C.; Mallouk, T. E.; Haushalter, R. C. *J. Mol. Struct.* **1998**, *470*, 49.

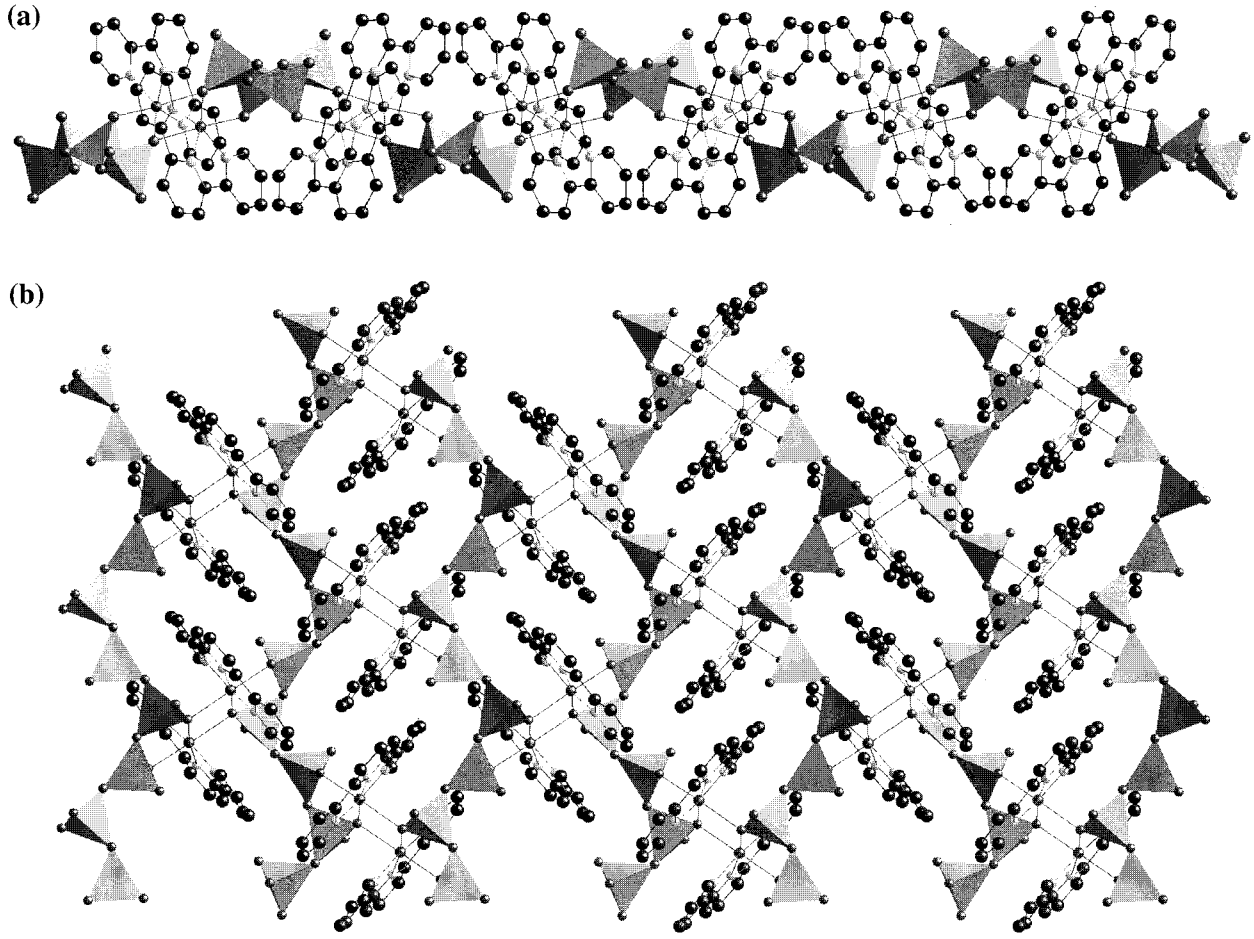

Figure 3. (a) The layer structure of **3** viewed along the *b* axis and (b) the layer of **3** as viewed along the crystallographic *c* axis.

bipyridine is used as the organic component, the compounds $[\{Zn(2,2'\text{-bpy})\}_2V_4O_{12}]$ (**1**) and $[Cu(2,2'\text{-bpy})V_4O_{10.5}]$ (**2**) were isolated. Blocking an additional coordination site on the secondary metal center by using a tridentate organonitrogen ligand, 2,2′:6′,2″-terpyridine, allowed the isolation of $[Cu(terpy)V_2O_6]$ (**3**) and $[\{Zn(terpy)\}_2V_6O_{17}]$ (**4**).

Experimental Section

All reagents were purchased from Aldrich Chemical Co. and were used without further purification. All syntheses were carried out under autogenous pressure with fill volumes of ca. 35% (preparations of **1**−**3** were carried out in borosilicate glass tubes while **4** was synthesized in a PTFE-lined Parr acid digestion bomb). The reactants were stirred briefly and heated. All water used was distilled above 3.0 Ω in-house using a Barnstead model 525 Biopure distilled water center.

Synthesis of $[\{Zn(2,2'\text{-bpy})\}_2V_4O_{12}]$ (1). A mixture of V_2O_5 (0.0515 g, 0.28 mmol), 2,2′-bipyridine (0.0239 g, 0.15 mmol), $ZnCl_2$ (0.0191 g, 0.14 mmol), and water (6.0149 g, 334 mmol) was placed in a borosilicate tube. To this mixture was added 0.2 mL of tetrabutylammonium hydroxide (40 wt % in water, TBAOH). The resultant slurry was stirred briefly, sealed, and heated at 200 °C for 7 days. Colorless crystals of **1** were isolated by mechanical separation from a mixture of **1** and unidentified black crystals. The yield of **1** was ca. 36% based on $ZnCl_2$.

Synthesis of $[Cu(2,2'\text{-bpy})V_4O_{10.5}]$ (2). A mixture of V_2O_5 (0.0480 g, 0.26 mmol), 2,2′-bipyridine (0.0222 g, 0.14 mmol), $CuCl_2{\cdot}2H_2O$ (0.0249 g, 0.14 mmol), and water (5.9061 g, 328 mmol) was placed in a borosilicate tube. Following the addition of 0.1 mL of TBAOH, the mixture was stirred, sealed in the tube, and heated at 200 °C for 92.5 h. Black crystals of **2** were isolated from a mixture of **2** and fine gold needles by mechanical separation. The yield of **2** was ca. 18% based on V_2O_5.

Synthesis of $[Cu(terpy)V_2O_6]$ (3). A mixture of V_2O_5 (0.0510 g, 0.28 mmol), 2,2′:6′,2″-terpyridine (0.0306 g, 0.13 mmol), $CuSO_4{\cdot}5H_2O$ (0.0690 g, 0.28 mmol), and water (5.0347 g, 280 mmol) were placed in a borosilicate tube and stirred briefly. After sealing, the tube was heated to 200 °C for 49.5 h. Blue plates of **3** were isolated from a mixture of **3** and an unidentified green solid. The yield of **3** was ca. 5% based on terpy.

Synthesis of $[\{Zn(terpy)\}_2V_6O_{17}]$ (4). A mixture of V_2O_5 (0.1089 g, 0.60 mmol), 2,2′:6′,2″-terpyridine (0.1385 g, 0.59 mmol), ZnO (0.0243 g, 0.30 mmol), and water (8.0099 g, 445 mmol) was placed in a polytetrafluoroethylene-lined Parr acid digestion bomb (fill volume 35%). The reaction mixture was heated to 210 °C for 135 h. Colorless blocks of **1** were isolated from a mixture of **1**, yellow powder, and striated red plates. The yield of **1** was ca. 21% based on ZnO.

X-ray Crystallography. Structural measurements for **1**−**4** were performed on a Bruker SMART-CCD diffractometer using graphite-monochromated Mo Kα radiation (λ(Mo Kα) = 0.71073 Å). The data for **1** and **2** were collected at a temperature of 120 ± 2 K while those for **3** and **4** were collected at 96 ± 2 K. All data were corrected for Lorentz and polarization effects. Data reduction was performed using SAINT, and an emprical absorption correction was made using SADABS.[20] The structures of **1**−**4** were solved via direct methods.[21] All non-hydrogen atoms in **1**−**4** were refined anisotropically. Neutral atom scattering coefficients and anomalous dispersion corrections were taken from *International Tables for Crystallography*, Vol. C.[22] All calculations were performed using the SHELXTL crystallographic software package.[21]

Crystallographic data for **1**−**4** are listed in Table 1. Atomic positional parameters and isotropic temperature factors for **1**−**4** are given in the

(20) *SAINT+*, version 6.02; Brüker AXS: Madison, WI, 1999.
(21) *SHELXTL*, version 5.1; Brüker AXS: Madison, WI, 1998.
(22) *International Tables for Crystallography*; Kluwer Academic Publishers: Dordrecht, 1989; Vol. C, Tables 4.2.6.8 and 6.1.1.4.

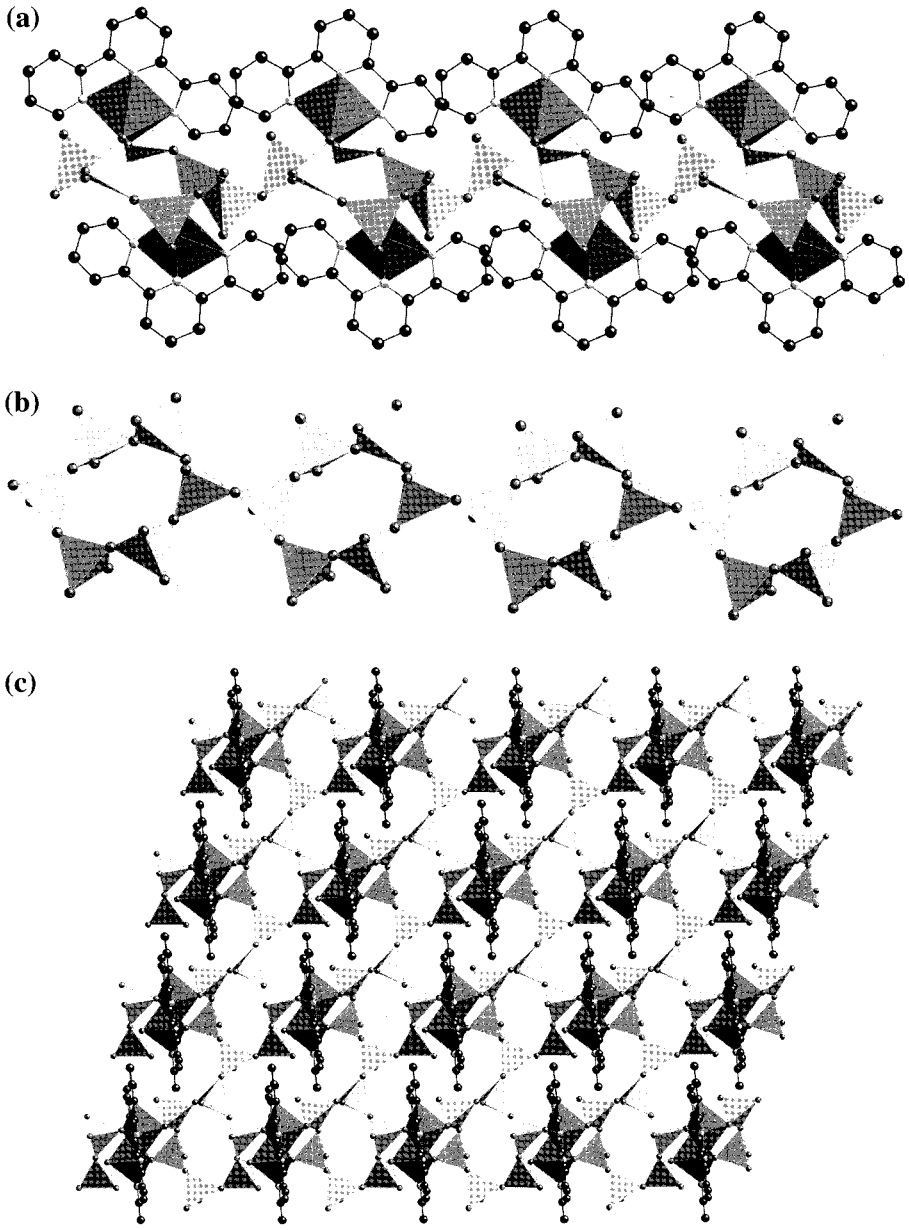

Figure 4. Polyhedral representations of compound **4** (a) as viewed along *b*, (b) illustrating the one-dimensional vanadate subunit of **4**, and (c) showing the layer structure of **4** as viewed perpendicular to the terpyridine ligands.

Supporting Information. Selected bond lengths and angles for **1**−**4** are listed in Table 2.

Results and Discussion

The exploitation of hydrothermal techniques has been shown to allow the isolation of metastable oxide phases. Moreover, combination of hydrothermal techniques with the introduction of organic substituents possessing structure-directing properties has resulted in the isolation of a series of related two-dimensional organic/inorganic materials exhibiting novel vanadium oxide substructures: $[\{Zn(2,2'\text{-bpy})\}_2V_4O_{12}]$ (**1**), $[Cu(2,2'\text{-bpy})V_4O_{10.5}]$ (**2**), $[Cu(terpy)V_2O_6]$ (**3**), and $[\{Zn(terpy)\}_2V_6O_{17}]$ (**4**). The hydrothermal syntheses of **1**−**3** were carried out in borosilicate glass tubes at a temperature of 200 °C while **4** was synthesized at 210 °C in a PTFE-lined Parr acid digestion bomb; all reactions were performed under autogenous pressures.

The hydrothermal technique utilized in these syntheses allows the isolation of phases which would be impossible to produce using conventional reflux temperatures or the ceramic method, and also lends itself to the retention of structural elements of the precursors used in the reaction, most importantly the organonitrogen component. Another important benefit of the choice of the hydrothermal method is that differential solubilities of the reactants, which are of some significance in this system due to low solubility of some starting materials, are less often a problem.[3]

As shown in Figure 1, the structure of **1** is a two-dimensional zinc vanadate layer with the 2,2′-bipyridine groups attached to the zinc centers directed above and below the plane of the layer. The layer is composed of rings containing four corner-sharing $\{VO_4\}$ vanadium(V) tetrahedra. These $\{V_4O_4\}$ units are linked through six zinc square pyramids to six adjacent $\{V_4O_4\}$ rings, as illustrated in Figure 1b, which depicts the layer of **1**. As is evident in Figure 1b, two of the vanadium tetrahedra in the ring corner share with one zinc square pyramidal unit each, while the other two vanadium tetrahedra within the ring each exhibit corner-sharing interactions with two zinc sites. Like vanadium tetrahedra are located on opposite sides of the ring. Each zinc

square pyramidal unit serves to link three V_4 rings through corner-sharing interactions. The zinc coordination sphere is completed by the nitrogens of the 2,2′-bipyridine ligand. The relative orientation of the 2,2′-bipyridine units with respect to the zinc vanadate layer is depicted in Figure 1a, which shows that the ligands are not oriented perpendicular to the plane of the layer but are instead canted at an angle of ca. 137° to the layer.

The structure of **2** is similar to that of **1** in that the gross topology is that of a two-dimensional material. In contrast to **1**, however, the layer of **2** is based on a two-dimensional vanadium oxide substructure while **1** was based on discrete $\{V_4O_4\}$ rings. The mixed-valence vanadium oxide layer of **2** is composed of vanadium(IV) square pyramids and vanadium(V) tetrahedra attached as shown in Figure 2. The arrangement of the 2,2′-bipyridine in **2** is such that the ligands form staggered stacks above and below the plane of the layer, with their orientation perpendicular to the layer when the structure is projected onto the *bc* plane in Figure 2a. However, viewing along the (−101) direction, as illustrated in Figure 2b, reveals that the bipyridine rings are tipped to form an angle of ca. 59.6° with the layer. The copper vanadate layer on which the structure is based is shown in Figure 2c. Evident in this view are serpentine subunits composed of six corner-sharing vanadium oxide tetrahedra, shown in darker gray. Each square pyramidal vanadium site, shown in lighter gray, links to three adjacent serpentine chains, one through two corner-sharing interactions and two through one corner-sharing interaction each. The apical oxo group of the vanadium square pyramid is oriented such that it points out from the vanadium oxide layer. Valence sum calculations[23] confirm that the square pyramidal site is present in the V(IV) oxidation state, resulting in a mixed-valence vanadium oxide layer substructure, as suggested by the intense color of **2**. In this synthesis, the reduction of the vanadium from the +5 to the +4 oxidation state is favored owing to appropriate pH and stoichiometry, with the bipyridine ligand presumably acting as a reducing agent. Each copper square pyramid attaches to three tetrahedra of the vanadium oxide layer through corner-sharing interactions. Two of these attachments are to vanadium tetrahedra from one serpentine unit while the third is to a vanadium tetrahedron from an adjacent serpentine unit. Each $\{V_6O_5\}$ chain of six corner-sharing vanadium tetrahedra is linked to six adjacent serpentines through six vanadium oxide square pyramids. The four copper square pyramids that link to each $\{V_6O_5\}$ unit provide further attachments to two of the six adjacent $\{V_6O_5\}$ strands to which the first is already attached via the $\{VO_5\}$ units. It should also be noted that the connectivity of the polyhedra observed in **2** is such that three distinct polyhedral vanadium oxide rings are formed, $\{V_2^{sq.pyr.}V_4^{tet.}O_6\}$, $\{V_2^{sq.pyr.}V_2^{tet.}O_4\}$, and $\{V^{sq.pyr.}V_4^{tet.}O_5\}$. The introduction of Cu(II) in place of Zn(II) leads to expected changes. The copper site of **2** shows four relatively short bonds, ranging from 1.941 to 1.996 Å, and one long Cu−O distance at 2.245 Å, resulting in (4 + 1) coordination as compared to the more regular five-coordinate Zn in **1** for which all Zn−O distances are in the range 2.013−2.116 Å.

Compound **3**, shown in Figure 3, is composed of one-dimensional vanadium oxide chains linked through copper−terpyridine units into a two-dimensional bimetallic oxide of composition $\{CuV_2O_6\}$. An edge-on view of the layer, shown in Figure 3a, reveals a shallow sinusoidal profile to the vanadium oxide layer, with a period of 16.3 Å, and an amplitude of approximately 7 Å. The one-dimensional vanadium oxide chain

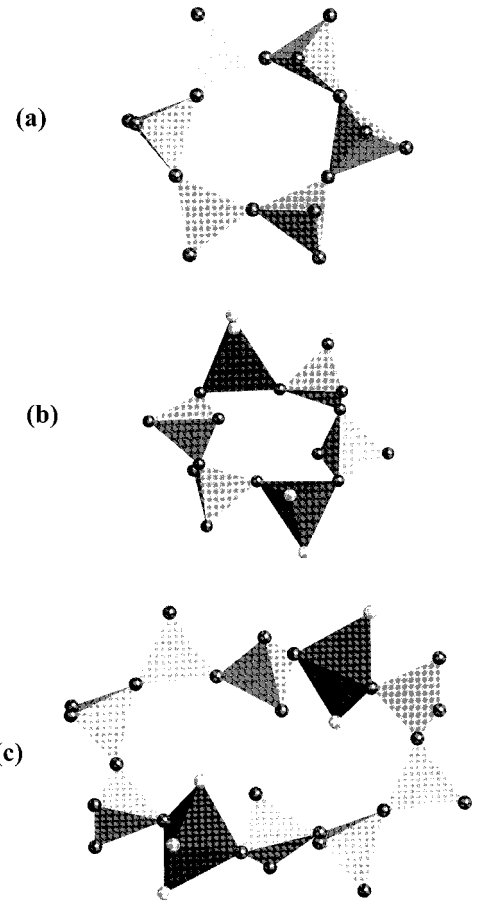

Figure 5. Polyhedral representations of the three distinct rings found in **4**: (a) a six-polyhedral vanadium oxide ring, (b) a six-ring containing two zinc and four vanadium polyhedra, and (c) a ten-polyhedral ring containing eight vanadium and two zinc centers.

of **3** is constructed from corner-sharing vanadium tetrahedra. There are two distinct vanadium centers in **3**, and the coordination geometries of each are tetrahedral. Both of these vanadium centers possess two bridging oxygen atoms which link to two adjacent vanadium oxide tetrahedra within the chain, and one terminal oxo group. However, as the fourth atom in its coordination sphere, one vanadium oxide center has a triply bridging oxygen which bridges to two copper sites while the other has a bridging oxygen which links to a single copper site.

Adjacent vanadium oxide chains are linked into a two-dimensional solid through copper binuclear units as shown in Figure 3b. Connectivity of the vanadium to the copper is through corner-sharing interactions of the copper octahedron with two adjacent tetrahedra in the chain. The coordination environment of the copper is best described as Jahn−Teller distorted "4 + 2" and consists of three nitrogens from the terpyridine ligand with Cu−N distances in the range 1.929−2.049 Å, two oxygens from one vanadium chain with bond distances of 1.919 and 2.369 Å, and a long interaction at 2.570 Å to an oxygen of the neighboring vanadium oxide chain. The copper sites of the binuclear unit exhibit edge-sharing interactions, and the coordination geometry of the copper is defined by three nitrogens from the 2,2′:6′,2″-terpyridine, one μ^3-oxygen from the vanadium oxide chain which also bridges to the adjacent copper octahedra, and a doubly bridging oxygen from the same vanadium oxide chain. The one-dimensional chain of corner-sharing tetrahedra, previously described for $[V_4O_{12}Cu_3$(1,2,4-

(23) Brown, I. D.; Altermatt, D. *Acta Crystallogr., Sect. C* **1985**, *41*, 244.

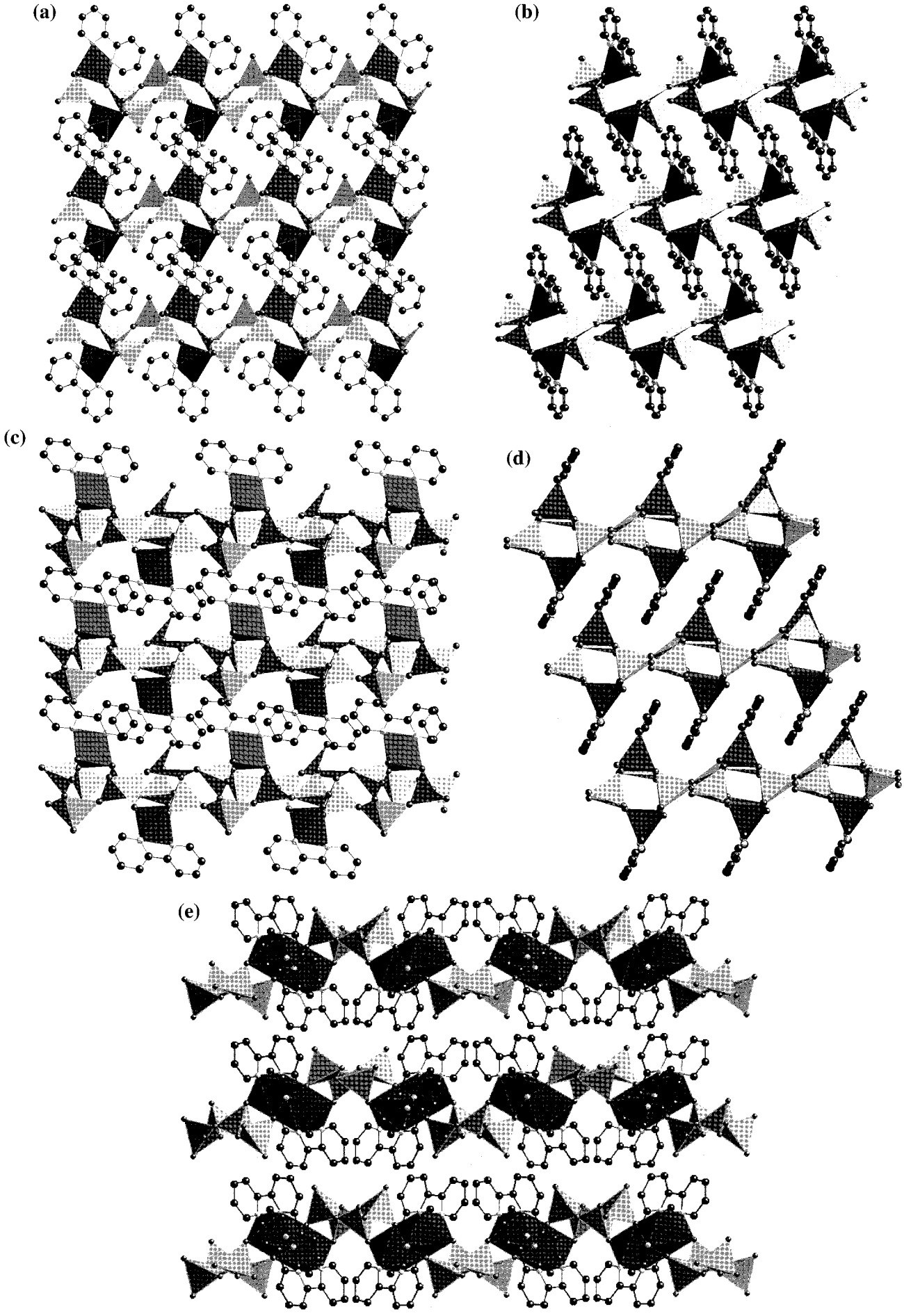
(a)
(b)
(c)
(d)
(e)

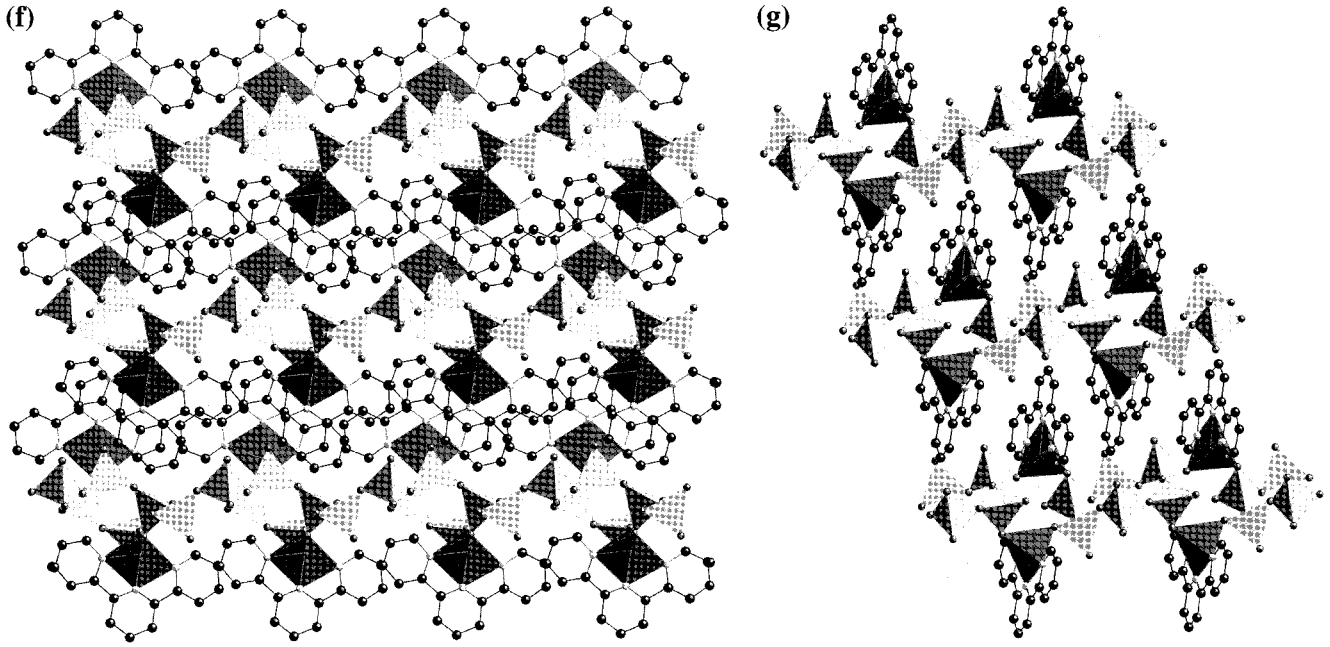

Figure 6. Views of the packing of (a) **1** viewed down *b*, (b) **1** viewed down *a*, (c) **2** viewed down *a*, (d) **2** viewed along [−1.5 0 1.5], (e) **3** viewed along *b*, (f) **4** viewed along *b*, and (g) **4** viewed down *c*.

triazole)$_2$],[24] is a building block also observed in the composite materials [Cu(bpy)][V_2O_6] and [Cu(bpy)$_2$][V_2O_6].[25]

The layer structure of **4**, shown in Figure 4a, is similar to that of **3** in that the vanadium oxide building blocks are one-dimensional chains which are linked into a layer through M(terpy)$^{2+}$ units. However, the chain units in **3** and **4** are distinctly different. Although both chains are composed solely of corner-sharing vanadium oxide tetrahedra, the chain seen in **3** is a single chain in which each tetrahedron corner shares with two similar adjacent tetrahedra, while the chain in **4** is more complex, being composed of fused rings of six corner-sharing vanadium oxide tetrahedra, as shown in Figure 4b. Each such six-ring is connected to two neighboring rings through additional corner-sharing interactions from two vanadium tetrahedra at opposite sides of the six-ring. Adjacent chains are linked into a two-dimensional structure through Zn(terpy)$^{2+}$ units as illustrated in Figure 4c.

There are two distinct types of connectivities of the vanadium tetrahedra in the ring. One type of vanadium serves to link adjacent six-rings, and possesses one terminal oxo group and three bridging oxygens which link that vanadium tetrahedron to three adjacent vanadium tetrahedra. The other type of vanadium coordination is to two oxygens which bridge to two adjacent vanadium tetrahedra, and one oxo group which links the vanadium tetrahedron to a zinc site. The coordination of the zinc site is defined by three nitrogens from the terpyridine ligand and two bridging oxygens from vanadium tetrahedra.

The layer of **4** contains three distinct types of rings. One type of ring is the aforementioned six-polyhedral vanadium oxide ring, shown in Figure 5a, which fuse to form the one-dimensional chains. A second six-ring, illustrated in Figure 5b, is also found which contains two zinc and four vanadium polyhedra. The third ring observed contains 10 polyhedra, with eight vanadium and two zinc centers within the ring, as shown in Figure 5c.

Stacking of adjacent layers of [{Zn(2,2′-bpy)}$_2$$V_4O_{12}$] (**1**), [Cu(2,2′-bpy)$V_4O_{10.5}$] (**2**), [Cu(terpy)$V_2O_6$] (**3**), and [$V_6O_{17}${Zn(terpy)}$_2$] (**4**) viewed edge-on, as illustrated in Figure 6, reveals differences in their relative packing arrangements and the overlap and interdigitation of the ligand rings. In the case of compound **1**, the 2,2′-bipyridyl groups interdigitate, as seen in Figure 6a, and there is some overlap of neighboring rings from adjacent layers, although the rings are somewhat staggered with respect to those on the adjacent layer. The interdigitation of the bipyridyl rings in **1** is depicted in Figure 6b, which also shows the canting of the rings with respect to the layer. Compound **2** exhibits overlap, but to a lesser extent than in **1**, as shown in Figure 6c. The interdigitation of **2** is depicted in Figure 6d. In contrast to the packing of **1** and **2**, compound **3** does not show interdigitation between adjacent layers, as illustrated in Figure 6e. The packing of **4**, shown in Figure 6f, shows considerable overlap of the terpyridine rings. Figure 6g reveals a high degree of interdigitation which is facilitated by the fact that the center rings of the terpyridine groups are directed toward the center of the six-polyhedral vanadium oxide rings within the layer.

Comparisons of **1**−**4** with the previously reported [{(2,2′-bpy)$_2$Zn}V_6O_{17}] and [{M(2,2′-bpy)}$_2$$V_{12}O_{32}$] (M = Co, Cu, Ni) illustrate the differences observed when the complex transition metal organic subunit is attached to molecular, one-dimensional, single-layer two-dimensional, or double-sheet oxide subunits. In the case of [{(2,2′-bpy)$_2$Zn}V_6O_{17}], the vanadium oxide layer on which the structure is based is a single-layer sheet composed of vanadium tetrahedra. This sheet exhibits large 14-ring holes within the layer with two fused Zn(2,2′-bpy)$_2$ groups per ring, located on opposite sides of the ring. In the case of [{M(2,2′-bpy)}$_2$$V_{12}O_{32}$] (M = Co, Cu, Ni), the two-dimensional vanadium oxide subunit is a vanadium oxide double sheet in which the divalent metal atoms occupy rectangular cavities.

Conclusions

The vanadium oxide subunits from which the two-dimensional structures of **1**−**4** are constructed are unlike those previously reported for the V/O/M(II) family of compounds.

(24) Hagrman, P. J..; Bridges, C.; Greedan, J. E.; Zubieta, J. *J. Chem. Soc., Dalton Trans.* **1999**, *17*, 2901.
(25) DeBord, J. R. D.; Zhang, Y.; Haushalter, R. C.; Zubieta, J.; O'Connor, C. J. *J. Solid State Chem.* **1996**, *122*, 251.

In the case of **1**, a $\{V_4O_4\}$ ring is the molecular "building block", while in **2** a unique two-dimensional sheet composed of fused vanadium square pyramids and tetrahedra serves as the scaffolding on which the structure is based. Compound **3** is based on a one-dimensional chain of corner-sharing vanadium oxide tetrahedra, while compound **4** is constructed from fused rings of six corner-sharing vanadium oxide tetrahedra. It is noteworthy that, while the one-dimensional chain of corner-sharing vanadium tetrahedra of **3** is unique, the chain observed in **3** does show some similarity to the vanadium oxide chain previously observed in $[V_4O_{12}Cu_3(1,2,4\text{-triazole})_2]$.

It is evident from examination of the previously published and newly reported compounds in which complex transition metal−organic units are incorporated into vanadium oxide structures that there is a great degree of variability in the vanadium oxide substructure on which these compounds are based. Vanadium oxide subunits ranging from molecular species, in the case of the $\{V_4O_4\}$ rings on which **1** is based, to double sheets which are the basis for $[\{M(2,2'\text{-bpy})\}_2V_{12}O_{32}]$ (M = Co, Cu, Ni) have now been observed. This structural variability reflects in part the polyhedral forms available to V(V) and V(IV) oxides, as well as the range of polyhedral connectivities which may evolve. The secondary metal−ligand component is involved in charge-compensation and space-filling roles, as well as providing a structure-directing component by virtue of the ligand geometry and steric constraints and the coordination preferences of the metal. While prediction of the overall structure of such complex hybrid materials remains elusive, further investigation into the interplay of such structural subunits in the construction of solids may allow the tailoring of magnetic and electronic properties of the layer for desired applications.

Acknowledgment. This work was supported by a grant from the National Science Foundation (CHE9987471).

Supporting Information Available: X-ray Crystallographic files in CIF format for **1**-**4**. ORTEPs for **1**−**4**. This material is available free of charge via the Internet at http://pubs.acs.org.

IC010024M